ACS OMEGA

Article

Cite This: ACS Omega 2019, 4, 19895−19904

http://pubs.acs.org/journal/acsodf

Continuous Activity Assay for HDAC11 Enabling Reevaluation of HDAC Inhibitors

Zsófia Kutil,[†] Jana Mikešová,[†] Matthes Zessin,[‡] Marat Meleshin,[§] Zora Nováková,[†] Glenda Alquicer,[†,⊥] Alan Kozikowski,[∥] Wolfgang Sippl,[‡] Cyril Bařinka,*[,†] and Mike Schutkowski*[,§]

[†]Institute of Biotechnology of the Czech Academy of Sciences, BIOCEV, Prumyslova 595, 252 50 Vestec, Czech Republic

[‡]Department of Medicinal Chemistry, Institute of Pharmacy, Martin-Luther-University Halle-Wittenberg, 06120 Halle (Saale), Germany

[§]Department of Enzymology, Institute of Biochemistry and Biotechnology, Charles Tanford Protein Centre, Martin Luther University Halle-Wittenberg, Kurt-Mothes-Straße 3a, 06120 Halle (Saale), Germany

[∥]StarWise Therapeutics LLC, 505 S Rosa Road, Suite 27, Madison, Wisconsin 53719-1235, United States

Supporting Information

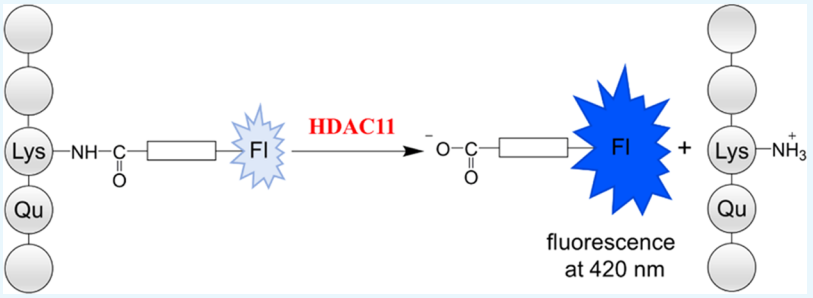

ABSTRACT: Histone deacetylase 11 (HDAC11) preferentially removes fatty acid residues from lysine side chains in a peptide or protein environment. Here, we report the development and validation of a continuous fluorescence-based activity assay using an internally quenched TNFα-derived peptide derivative as a substrate. The threonine residue in the +1 position was replaced by the quencher amino acid 3′-nitro-L-tyrosine and the fatty acyl moiety substituted by 2-aminobenzoylated 11-aminoundecanoic acid. The resulting peptide substrate enables fluorescence-based direct and continuous readout of HDAC11-mediated amide bond cleavage fully compatible with high-throughput screening formats. The Z'-factor is higher than 0.85 for the 15 μM substrate concentration, and the signal-to-noise ratio exceeds 150 for 384-well plates. In the absence of NAD^+, this substrate is specific for HDAC11. Reevaluation of inhibitory data using our novel assay revealed limited potency and selectivity of known HDAC inhibitors, including Elevenostat, a putative HDAC11-specific inhibitor.

INTRODUCTION

Reversible ac(et)ylation of lysine side chains has emerged as one of the major regulatory mechanisms in living organisms. It is involved in the modulation of protein−protein interactions, protein localization and degradation, and moreover in chromatin assembly, DNA repair, and metabolic stress response. Acyl residues are introduced either by the action of acetyltransferases using acyl-CoAs as cosubstrates or by spontaneous reactions of acyl-CoA thioesters with the lysine side chains. In the past 10 years, other types of acyl modifications, propionylation,[1] butyrylation,[1] malonylation,[2,3] succinylation,[4] glutarylation,[5] crotonylation,[6] 3-hydroxybutyrylation,[7] 4-oxo-nonaoylation,[8,9] hydroxyisobutyrylation,[10] 3-hydroxy-3-methyl-glutarylation,[11,12] 3-methyl-glutarylation,[11,12] 3-methyl-glutaconylation,[11,12] 3-phosphoglycerylation,[13] benzoylation,[14] myristoylation,[15] and stearoylation[16] have been identified, thereby dramatically expanding the portfolio of post-translation modifications controlling a number of cellular processes.[17,18]

Removal of acyl residues from lysines is catalyzed by histone deacetylases (HDACs). This reaction is more tightly regulated by the substrate and acyl specificities of individual HDACs and their spatiotemporal distribution within the cell. HDACs are evolutionarily conserved among organisms. Based on sequence homology and enzymatic mechanism, HDACs can be divided into 4 classes. Members of classes I (HDAC 1, 2, 3, and 8), II (HDAC4−7, 9 and 10), and IV (HDAC11) are Zn^{2+}-dependent hydrolases, while class III proteins (called sirtuins; SIRT 1−7) use NAD^+ as the cosubstrate for the transfer of the acyl moiety from the lysine side chain to the ADP-ribosyl fragment of NAD^+ generating nicotinamide as the third product of the reaction.[19] Recently, our group and others identified a robust defatty acylase activity for HDAC11,[20−22] which may represent the major enzymatic activity of HDAC11

Received: August 30, 2019
Accepted: October 18, 2019
Published: November 15, 2019

DOI: 10.1021/acsomega.9b02808
ACS Omega 2019, 4, 19895−19904

in vivo. HDAC11 is involved in the regulation of the immune system and the modulation of cancer growth,[19,23] and very recently, it has been demonstrated that HDAC11 knock-out protects mice from high-fat diet-induced obesity and metabolic syndrome,[24] making HDAC11 an interesting target for the treatment of cancer and obesity-related diseases.

There is only limited information on the development and use of HDAC11-specific inhibitors. In 2017, Huang et al. reported Elevenostat (compound JB3-22), the putative HDAC11-specific inhibitor, to be effective in pharmacologic modulation of functions of T-regulatory cells.[25] Very recently, the development of FT895, a hydroxamate-based small-molecule compound, has been described by Martin et al.,[26] and 2-carboxamidothiophene-based zinc ion chelating carbohydrazides were shown to be selective HDAC11 inhibitors active in vivo.[27] Additionally, several pan-HDAC inhibitors used in clinical trials, including romidepsin and trichostatin A (TSA), are reported to have nanomolar potency for HDAC11. At the same time, however, inhibitory constants of these and other small molecules toward HDAC11 listed in the ChemBL database are somewhat inconsistent, and these inconsistencies may stem from different assay conditions (pH values, the presence of additives like bovine serum albumin (BSA) or detergents, and substrate concentrations) as well as the use of suboptimal substrates like acetylated peptides, which are very poorly accepted by HDAC11. Consequently, we believe that reevaluation of some of these findings would be valuable for the scientific community focused on biological experiments in the future.

The detection of HDAC activity is often coupled to a separation of a substrate and its reaction product. Different methods are used for such separation steps, including capillary electrophoresis,[28] microchip electrophoresis,[29] microfluidic mobility assay,[30,31] polyacrylamide gel electrophoresis,[32] high-performance liquid chromatography (HPLC),[33−36] thin-layer chromatography,[37] charcoal-binding,[38] binding to boronic acid resins,[39] and extraction with organic solvents.[40] Owing to this additional separation step, the resulting assay format is discontinuous and not suited for high-throughput applications. Alternatively, mass spectrometry could be used for the separation of the substrate and the reaction product.[41,42] Matrix assisted laser desorption ionization-time of flight mass spectrometry readout, in combination with peptide derivatives immobilized on glass surfaces, was used for the systematic profiling of substrate specificity of HDAC2, HDAC3, and HDAC8.[43,44] Additionally, HDAC activity patterns could be determined in cell lysates using this technique.[45] Moreover, the same technology uncovered the dependence of the HDAC8 substrate specificity on the nature of the metal ion within the active site.[46] Alternative approaches make use of reagents sensing either the acetylated substrates, like acetyllysine recognizing antibodies,[47−52] or the reaction products. The release of radioisotopically labeled acetate was used to analyze HDAC activity.[53−56] More recently, acetate could be captured by coupling to an enzymatic reaction,[57] and a chemical reaction was used to trap the HDAC8-mediated release of thioacetate yielding a chromophore.[58] Reagents for the detection of the generated primary amine in the peptide product could either be chemicals, like biotin-containing active esters or activated fluorescent dyes, reacting with the lysine side chain[59,60] or intramolecular reactions, like transesterification with a coumarin dye,[61] which is only possible if the lysine side chain is released by HDAC activity.[62−65] Additionally, aggregation-induced emission[66,67] and modulation of binding to DNA[68,69] were used to probe HDAC activity.

An interesting alternative is the coupling of the HDAC-mediated reaction to a proteolytic reaction using proteases, specific for the free lysine side chain in the reaction product.[34,56,70,71] The fluorescence-based readout for the proteolytic reaction is common to increase the sensitivity of the assay. Commercially available HDAC substrates are fused to 7-amino-4-methylcoumarin, resulting in bright fluorescence subsequent to cleavage of the lysinyl-coumaryl amide bond.[72−78] However, as the proteolytic stability of different HDACs against the developer proteases is limited, most protease-coupled HDAC assays have to be performed in a discontinuous manner. The additional disadvantage stems from the fact that the substituted coumaryl moiety represents an artificial residue within the HDAC substrate preventing the investigation of substrate specificities in +1, +2, etc. positions. Moreover, it was demonstrated that profiling of HDAC activity with substrates containing coumaryl fluorophores yielded results different from screening results with more natural substrates, including artificially enhanced affinity to the active site (HDAC6) or loss of sequence specificity (HDAC4).[79] Additionally, substrates of this type are characterized by suboptimal K_M-values in the high micromolar range.

Continuous assays without coupling to enzymatic or chemical reactions are described for sirtuins.[80,81] In these cases, a fluorophore or a quencher is an integral part of the acyl moiety linked to the lysine side chain. Such an approach is not feasible for HDACs of classes I and II because their narrow acyl binding pockets cannot accommodate acyl groups decorated with bulky fluorophore moieties. In contrast, HDAC11 is able to remove hydrophobic, long-chain acyl residues from lysine side chains,[20−22] and therefore, we wondered if continuous substrates described for sirtuins are suitable for the determination of HDAC11 activity. Here, we report the development of a continuous and direct activity assay for HDAC11 based on internal fluorescence quenching. Using this novel HDAC11 activity assay in comparison to the data generated using a commercially available trifluoroacetylated lysine derivative, we were able to reevaluate the potency of known HDAC inhibitors including Elevenostat, Pracinostat, Quisinostat, Dacinostat, Trapoxin A, and Romidepsin. Additionally, we were able to demonstrate that this HDAC11 activity assay is fully compatible with high-throughput screening formats.

RESULTS

Continuous and Direct Activity Assay for HDAC11. HDAC11 is able to remove decanoyl, dodecanoyl, and myristoyl residues from lysine side chains in the sequence context of a substrate sequence derived from peptide microarray experiments.[22] We wondered if the active site of HDAC11 could adopt an aminoundecanoic acid residue, which is acylated by anthranilic acid. In the past, we were able to demonstrate that such modification of the acyl moiety is well tolerated by most of the class III HDACs (sirtuins).[81] Fluorescence of the anthraniloylamide is efficiently quenched by a 3-nitrotyrosine residue in the +1 position of a TNFα-derived peptide substrate 1, resulting in an increase of fluorescence subsequent to HDAC11 treatment (Figure S2). We used substrate 1 (see Figure 1) because it is derived from a known in vivo myristoylation site.[82] First, we analyzed the substrate properties using human HDAC11 in combination

DOI: 10.1021/acsomega.9b02808
ACS Omega 2019, 4, 19895−19904

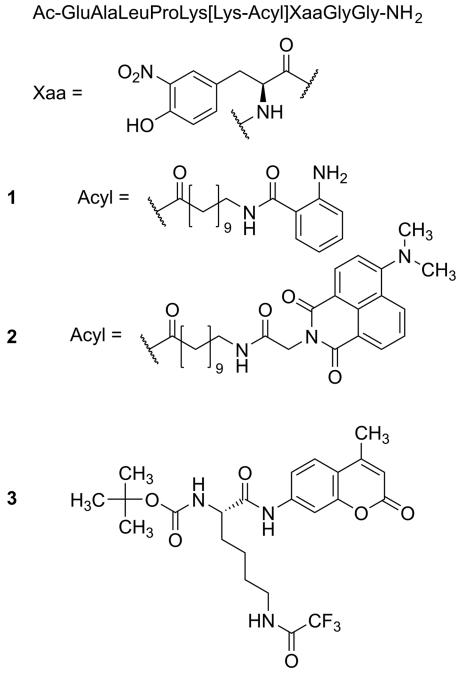

Figure 1. General structure of the substrates. Peptide substrates 1 and 2 were derived from the known myristoylation site TNFα-Lys20.[15] The naturally occurring threonine residue in +1 position is replaced by the quencher L-3-nitrotyrosine. The lysine side chain corresponding to Lys20 of TNFα is acylated with fluorescent N-anthraniloylated (peptide 1) or N-(4-*N*,*N*-dimethylamino-1,8-naphthalimido)acetyl (peptide 2) 11-aminoundecanoic acid. Lysine derivative 3 represents the commercially available trifluoroacetylated HDAC substrate.

with an HPLC-based assay as described.[20] Substrate 1 is well accepted by HDAC11 with a specificity constant very similar to the values for trifluoroacetylated substrates used in protease-coupled assay formats. To increase the wavelength used for the excitation of fluorescence, we generated peptidic substrate 2 (Figure 1) equipped with a sterically more demanding fluorophore. Using an HPLC-based activity assay, we were able to demonstrate the cleavage of the amide bond at the side chain of the lysine residue but with very poor kinetics (Figure S3). After treatment with 500 nM HDAC11 for 1 h, around 6% substrate conversion could be detected. Obviously, the hydrophobic pocket of HDAC11 accepting the acyl lysine is sensitive to sterically more demanding moieties, at least at the distal positions.

When fluorescence change was monitored over time, the resulting progress curves at different concentrations of HDAC11 were linear up to 25% conversion of the substrate. In the absence of HDAC11, a slight fluorescence decrease of 7% of the total fluorescence intensity is detectable after 30 min (Figure 1a). The slope of the fluorescence increases of reaction solutions containing 1 and HDAC11 is dependent on the enzyme concentration, resulting in a linear correlation between the HDAC11 amount and the reaction rate (Figure 1b). This dependence on enzyme concentration demonstrates that the measured signal increase is caused by the enzyme-mediated cleavage of the amide bond and not by fluorescence artifacts. Therefore, peptide derivative 1 could be used for the recording of HDAC11 activity in a continuous format. For the generation of appropriate calibration curves, *N*-(2-aminobenzoyl)-11-aminoundecanoic acid, the reaction product, was used. We found a pronounced dependence of HDAC11 activity on the concentration of bovine serum albumin (BSA) in the assay buffer (Figure 2c). Therefore, all measurements were performed in the presence of 2 mg/mL of BSA. To ensure that this concentration of BSA does not affect the inhibitor's potency, we have tested the quisinostat as a representative of moderately active inhibitors in different concentrations of BSA in the buffer. No decisive effect of BSA on the activity of the inhibitor was observed at concentrations tested (Supporting Information Figure S5). To demonstrate that the activity assay is useful for high-throughput screenings, we performed measurements in 96-, 384-, and 1536-well microtiter plates (Figure 2d) yielding excellent Z'-factors of 0.85 for 1 at 15 μM concentration. The K_M values determined using the different microtiter plate formats are very similar, and the resulting specificity constants are in the range of 11 000 to 13 000 M^{-1} s^{-1} (Figure 2).

Because HDAC8 is the only other Zn^{2+}-dependent HDAC, which is able to accept longer acyl moieties, we tested peptides 1 and 2 as HDAC8 substrates using an HPLC-based activity assay. We found less than 1% cleavage using 500 nM HDAC8 for 4 h, with a 20 μM peptide substrate. Thus, in the absence of NAD^+, which prevents any action of sirtuins against 1, peptidic substrate 1 could be considered as an HDAC11-specific substrate.

Reevaluation of known HDAC Inhibitors Using Peptidic Substrate 1 and Trifluoroacetyllysine Derivative 3. Most of the typical HDAC inhibitors are not active against HDAC11. Nevertheless, several inhibitors were described for HDAC11 with IC_{50} values in the low nanomolar range. Trapoxin A is an inhibitor of HDAC11 activity with an IC_{50} value of 170 nM and a K_i value of 24 nM if a myristoylated peptidic substrate was used for activity measurements. We determined the IC_{50}-value for Trapoxin A-mediated HDAC11 inhibition using 1 to validate the continuous and fluorescence-based activity assay. We found an IC_{50} value of 10 nM (Table 1), which is in good agreement with the data from the literature. TSA is an inhibitor for HDAC11 with described affinities between 14 nM[83] and 32 μM.[21] If measured with an acetylated fluorogenic pentapeptide derived from p53, an IC_{50} value of 17 nM was reported.[84] In contrast, no efficient inhibition by TSA could be detected using a myristoylated peptidic derivative with an estimated IC_{50} value of 32 μM.[21] We used 1 to reanalyze the effect of TSA on HDAC11 activity and obtained less than 50% inhibition at 20 μM inhibitor resulting in an IC_{50} of 22 μM (Table 1). This demonstrates that substrate 1 yielded results closer to results found using myristoylated substrates. For comparison, we profiled TSA-mediated inhibition of HDAC11 with the trifluoroacetylated lysine derivative 3 and again found no effective inhibition (an IC_{50} value of 10 μM). Similarly, we analyzed romidepsin, a cyclic peptidic inhibitor used in the clinic. An IC_{50} value of 0.3 nM[85] could not be confirmed using either substrate 1 or 3 (Table 1). In our hands, romidepsin is active against HDAC11 with the IC_{50} value in the low μM range. This finding is supported by the reported IC_{50} value of higher than 10 μM if a trifluoroacetylated substrate peptide was used.[86] To our surprise, several inhibitors that are described to be highly efficient against HDAC11, like Dacinostat, Elevenostat, Pracinostat, Mocetinostat, and Quisinostat, are not so effective if analyzed using substrates 1 and 3 (Table 1). In all cases, the reported values were generated using acetylated substrates. On the other hand, we were able to confirm the efficient inhibition of HDAC11 by fimepinostat using substrate 1, demonstrating

DOI: 10.1021/acsomega.9b02808
ACS Omega 2019, 4, 19895−19904

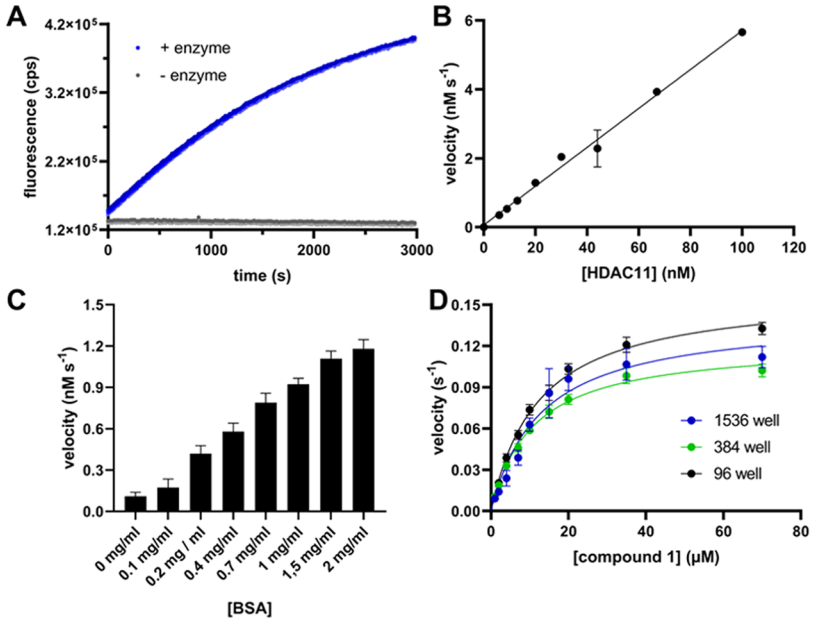

	96 well	384 well	1536 well
k_{cat} (s^{-1})	0.16 ± 0.004	0.122 ± 0.006	0.142 ± 0.001
K_M (μM)	12.2 ± 0.2	10.7 ± 1.1	12.7 ± 1.8
k_{cat}/K_M ($s^{-1}M^{-1}$)	13052	11474	11140

Figure 2. Fluorescence measurements using substrate 1. (A) Fluorescence change as a function of time. The excitation/emission wavelengths were set at 330 ± 75/430 ± 8 nm, respectively. The reaction was performed with the 15 μM substrate and 30 nM HDAC11 (blue dots) as well without enzyme (gray dots). (B) Fluorescence change as a function of the HDAC11 concentration. The reactions were performed with 100, 67, 44, 30, 20, 13, 9, and 6 nM HDAC11 and 50 μM substrate. (C) Velocity of the product formation as a function of BSA concentration in the buffer. The substrate concentration (peptide 1) was 20 μM and HDAC11 concentration was 30 nM. The experiment was performed once with n = 6, and the error bars show the standard deviation (SD). (D) Steady-state kinetics of HDAC11 with compound **1**. Reactions were performed using 30 nM HDAC11 and varying concentrations of 1 (0.1−70 μM). The results are from two independent experiments, and each experiment was done with n = 3 (96 well), n = 4 (384 well), and n = 6 (1536 well) replicates, and the error bars show the standard deviation. The velocity v means product formation per time unit and per active site. The resulting kinetic constants of the fit are summarized in the table below.

that 1 is suitable for inhibitor screenings resulting in less false positives compared to screenings with acetylated substrates.

DISCUSSION

HDAC11 is one of the least studied HDAC isoforms. To evaluate its biological function, highly efficient tools are needed, like compound selectively inhibiting HDAC11 with high affinity. Screening of large compound libraries is limited by the complex assays known for HDAC activity measurements. Most of the fluorogenic assays are discontinuous because of the limited stability of the HDACs against the developer protease used. Alternative assays, like HPLC-based or MS-based formats, are very time consuming, and therefore not suited for HTS applications. Moreover, HDAC11 is unique in the sense of substrate specificity. It has very poor activity against acetylated substrates but robust activity on trifluoroacetylated substrates and substrates with decanoylated or myristoylated lysine side chains. Based on this knowledge, we developed peptidic substrate 1, which is from the structural point of view closer to the myristoylated in vivo substrates. We then used this substrate to reevaluate some of the HDAC inhibitors, especially compounds described to be efficient against HDAC11 (Table 1, Figure 3). There are two major findings. First, effective inhibitors identified using either trifluoroacetylated substrates (Fimepinostat)[87] or myristoylated substrates (Trapoxin A[21]) could be confirmed using substrate 1. Second, effective compounds identified using acetylated substrates are not so effective if analyzed using either 1 or 3 (Table 1). The very poor activity of HDAC11 against acetylated substrates generates a problem if the enzyme preparation is contaminated with traces of HDACs that are highly active against acetylated substrates. Such contaminations are probably because most of the commercially available HDAC11 preparations have suboptimal purity. Depending on the respective kinetic constants, contaminating HDAC amounts less than 0.1 percent (which is hardly visible in PAGE gels) could generate a robust signal leading to false-positive screening hits. This situation is better if trifluoroacetylated substrates are used because HDAC11 is more active in such cases. Nevertheless, other HDACs like HDAC4, 5, 7, 8, and 9 are known to recognize trifluoroacetyllysine substrates with substantially higher efficacy. Substrate 1 is optimal for HDAC11 measurements because this is the only isoform that is able to handle this acyl moiety. In principle, sirtuins 1−6 can deacylate substrate 1, but for that reaction, the presence of the NAD^+ cosubstrate is necessary.[81]

Careful inspection of the presented IC_{50} values in Table 1 uncovers higher IC_{50} values for measurements performed with substrate 1 compared to lysine derivative 3 resulting in up to 5-

DOI: 10.1021/acsomega.9b02808
ACS Omega 2019, 4, 19895−19904

Table 1. IC_{50} Values for Listed Inhibitors were Determined Using the Peptidic Substrate 1 (15 μM of 1 and 20 nM HDAC11) and Lysine Derivative 3 (10 μM 3 and 60 nM HDAC11) and Compared to IC_{50} Values found in the Literature

compound	compound class	IC_{50} (nM) peptide derivative 1	IC_{50} (nM) lysine derivative 3	IC_{50} (nM) reported
dacinostat (NVP-LAQ824)	hydroxamic acids	9400 ± 1200	3930 ± 80	5.6[93]
elevenostat (JB3-22)	hydroxamic acids	17 700 ± 2700	5810 ± 470	235[25]
fimepinostat (CUDC-907)	hydroxamic acids	23 ± 3	16 ± 7	5.4[87]
mocetinostat (MGCD0103)	benzamides	>40 000	>40 000	590;[94] 195[95]
nexturastat A	hydroxamic acids	>40 000	8330 ± 1780	
pracinostat (SB939)	hydroxamic acids	34 800 ± 10 800	28 000 ± 360	93[96]
quisinostat (JNJ-26481585)	hydroxamic acids	3270 ± 280	1770 ± 270	0.37[95]
ricolinostat (ACY1215)	hydroxamic acids	12 300 ± 1700	5380 ± 360	>10 000[97,98]
romidepsin (FK228)	cyclic peptides	2700 ± 60	4810 ± 40	0.3;[85] >10 000[86]
trapoxin A	cyclic peptides	10 ± 1.4	78 ± 2	170[21]
trichostatin	hydroxamic acids	22 000 ± 6800	10 300 ± 1900	14;[83] 17;[84] 25;[99] 31;[100] 15;[101] 32 000[21]
valproate	aliphatic acids	>40 000	>40 000	

fold differences. These differences are smaller if the respective K_i-values are calculated because of the much better K_M value of substrate 1 (Figure 4, Table S3). Additionally, differences in inhibition constants depending on the chemical nature of the used substrate are known in the field of sirtuin research[88] and for HDAC8. Sippl et al. were able to demonstrate that IC_{50} values can differ up to 10-fold, depending on the used substrate.[89]

In summary, we developed an efficient and HDAC11-selective substrate enabling high-throughput screening of inhibitor libraries yielding reduced false-positive hits.

MATERIALS AND METHODS

Chemicals. All chemicals were purchased from Sigma (Saint Louis) if not denoted otherwise. Trifluoroacetic acid (TFA) was obtained from Roth (Karlsruhe, Germany). Peptidic substrate 1 is commercially available from JPT Peptide Technologies (Berlin, Germany) and lysine derivative 3 was purchased from Bachem (Bubendorf, Switzerland; #4060676).

The synthesis of all peptidic substrates is described.[20,81] HDAC inhibitors were purchased from Selleckchem and Cayman Chemical.

HDAC11 Expression and Purification. Full-length human HDAC11 was expressed and purified as described previously.[20] Briefly, HDAC11 was expressed using HEK-293/T17 cells following transient transfection mediated by linear polyethylene imine (PEI; Polysciences Inc., Warrington, PA). Three days after transfection, cells were harvested by centrifugation at 500g for 10 min and suspended in a lysis buffer (50 mM Tris, 150 mM NaCl, 10 mM KCl, 2 mM $MgCl_2$, 10% glycerol, pH 8) supplemented with benzonase (2 U/mL; Merck, Darmstadt, Germany) and a cocktail of protease inhibitors (Roche, Basel, Switzerland). Cell lysis was enhanced by the addition of Igepal-630 (final concentration 0.2%), followed by incubation for 30 min at 4 °C. The cell lysate was cleared by centrifugation at 40 000g for 30 min at 4 °C, and the supernatant was loaded on a Strep-Tactin column (IBA, Gottingen, Germany) previously equilibrated in the lysis buffer. The column was first washed with the lysis buffer supplemented with 2 mM ATP and 10 mM $MgSO_4$, followed by the second wash with the elution buffer (50 mM 4-(2-hydroxyethyl)-1-piperazineethanesulfonic acid (HEPES), 100 mM NaCl, 50 mM KCl, 10% glycerol, pH 7.5). Fusion proteins were eluted with the elution buffer supplemented with 3 mM desthiobiotin. Eluted proteins were concentrated to 2 mg/mL and flash-frozen in liquid nitrogen.

Continuous Fluorescence Assay. The assay was carried out as described previously with a slight modification.[81] The fluorescence measurements were performed using a fluorescence spectrophotometer CLARIOstar (BMG Labtech GmbH, Ortenberg, Germany) at λ_{ex} = 310 nm and λ_{em} = 405 nm. The reaction mixture consisted of HDAC11, and the substrate in a reaction buffer comprising 50 mM HEPES, 140 mM NaCl, 10 mM KCl, 2 mg/mL BSA, and 1 mM TCEP, at pH 7.4 was adjusted with NaOH (total volume 50 μL). The reactions were incubated in black 384-well plates for 60 min at 37 °C, and the increase of relative fluorescence reflecting the product formation was monitored. This signal was converted into product concentration via calibration curves of free *N*-(2-aminobenzoyl)-11-aminoundecanoic acid, the product of the reaction. For the determination of kinetic constants, 20 nM HDAC11 and the substrate in the concentration range of 0.04−200 μM were used. The slope of the linear regression of product formation against time yielded the reaction velocity rates in μM/s. Kinetic constants (K_M and k_{cat}) were obtained by nonlinear regression analysis according to Michaelis−Menten.

HPLC-Based Assay. The determination of kinetic constants and IC_{50} values of inhibitors was carried out in parallel to the continuous fluorescence assay by discontinuous assays analyzed by means of reversed-phase high-performance liquid chromatography (RP-HPLC). The reaction buffer, concentration of enzyme, substrates, and inhibitors were carried out as described above. The reaction was quenched by the addition of 0.5% acetic acid after 30 min of incubation and centrifuged at 2000g at 37 °C for 15 min to remove precipitated BSA and HDAC11. The reactions were analyzed by RP-HPLC (Shimadzu, HPLC Prominence system) with a Kinetex 2.6 μm XB-C18 100 Å column (100 × 3 mm; Phenomenex, Torrance, CA). The mobile phase A was 5% acetonitrile with 0.1% (v/v) TFA and the mobile phase B was 95% acetonitrile with 0.1% (v/v) TFA. The separation of the reaction product from the acylated substrate was performed in a 12-min linear gradient from 10 to 60% of eluent B at a flow rate of 0.6 mL/min. The product and substrate peaks were quantified using the absorbance at 365 nm (absorption of the 3-nitrotyrosyl moiety) to verify the results of the fluorescence assay.

Discontinuous Fluorescence-Based Assay using Boc-Lys(TFA)-7-amino-methylcoumarylamide Derivative. The assay was carried out using the commercially available substrate 3 as described previously with a slight modification.[90] Briefly, 60 nM HDAC11 was incubated with an inhibitor in the concentration range of 0.006−100 000 nM. The reaction was started with the 10 μM substrate and quenched after 30 min at

DOI: 10.1021/acsomega.9b02808
ACS Omega 2019, 4, 19895−19904

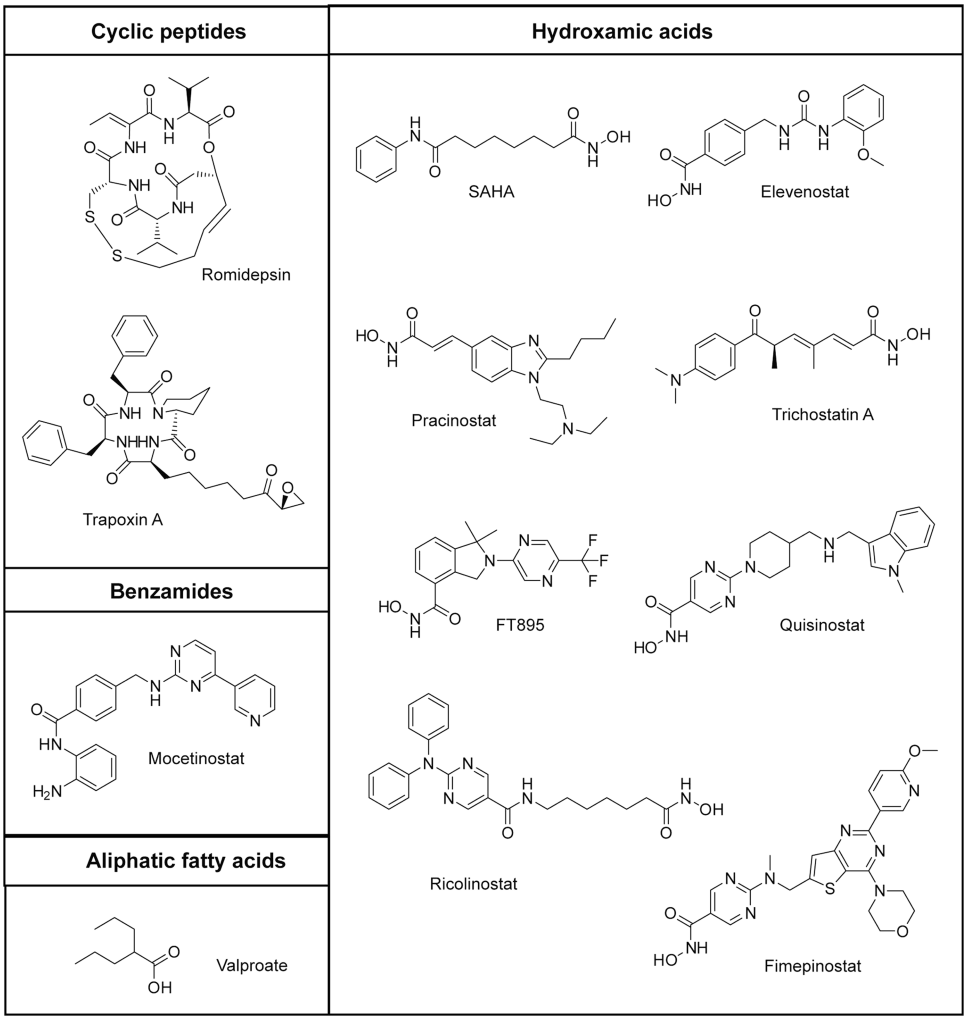

Figure 3. Structures of inhibitors used in this study.

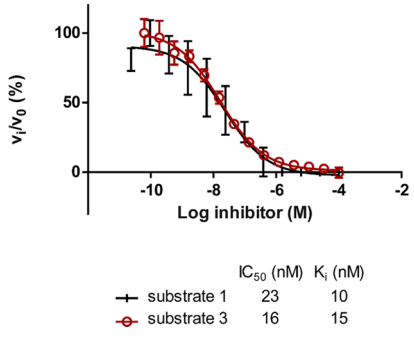

Figure 4. Determination of IC_{50} values for CUDC-907 using substrates 1 and 3. K_i-values were calculated with the Cheng−Prusoff relationship.[102] The K_M-value used for the calculation for compound **1** was 12 μM and for compound **3** 200 μM.

37 °C by the addition of 20 μL of trypsin solution (2 mg/mL trypsin, 20 mM Tris−HCl, 150 mM NaCl, 1 mM EDTA; pH 7.4). Following the 60 min incubation at 37 °C, a fluorescence signal of released aminomethylcoumarin was quantified using a CLARIOstar fluorimeter (BMG Labtech GmbH, Ortenberg, Germany) with excitation/emission wavelengths set at 365/440 nm, respectively.

Determination of Inhibition Constants. For the determination of IC_{50} values, 20 nM HDAC11 was preincubated 10 min with an inhibitor in the concentration range of 0.006−100 000 nM, and the reaction was started by the addition of 15 μM of substrate 1. The data were fitted using GraphPad Prism software, and IC_{50} values were calculated by nonlinear regression analysis. The inhibitor-free and enzyme-free controls were defined as 100 and 0% HDAC11 activity, respectively. All measurements were performed in duplicates.

Determination of Kinetic Constants. The assay was carried out as described previously with a slight modification.[91] The fluorescence measurements were performed with an EnVision 2104 Multilabel reader (Perkin Elmer, Waltham). An excitation filter with λ = 330 ± 75 nm and an emission filter with λ = 430 ± 8 nm (percent of excitation light = 2%, detector gain = 50, flashes per A/D conversion = 1, and number of flashes = 30). The reaction mixture containing peptide 1 in various concentrations and assay buffer (20 mM phosphoric acid pH 7.4 adjusted with NaOH and 2 mg/mL BSA) was incubated at 25 °C in a 96-well plate for at least 5 min. The reaction was started with the addition of HDAC11 to a final concentration of 30 nM and a total volume of 100 μL per well. For the measurements in the 384-well plate and the 1536-well plate, the reaction mixture (composition like above) was incubated for at least 5 min in a clear 96-well plate. The reaction was started with the addition of HDAC11, and the reaction mixture with the enzyme was transferred to the

DOI: 10.1021/acsomega.9b02808
ACS Omega 2019, 4, 19895−19904

-appropriate well plate (384-well plate with 20 μL per well and 1536-well plate with 9 μL per well). The increase of relative fluorescence intensity reflecting product formation was monitored and the signal was converted via calibration lines of free *N*-(2-aminobenzoyl)-11-aminoundecanoic acid, the fluorescent product of the reaction. For the determination of kinetic constants, 30 nM HDAC11 and the substrate in the concentration range of 0.04−70 μM were used. The initial slope of the linear regression of product formation against time yielded the reaction velocity rates in μM/s. Kinetic constants (K_M and k_{cat}) were obtained by nonlinear regression according to Michaelis−Menten.

***Z′* Factor Determination.** The *Z′*-factor is a dimensionless statistical parameter for high-throughput screening assays.[92] The *Z′*-factor was calculated from the mean of the initial slope from the change of the fluorescence intensity over time with 15 μM peptide 1 and 30 nM HDAC11 (mean (100%)). The negative control was determined in the same way without enzyme (mean (0%)). The standard deviation (SD) was calculated from 3 technical replicates (96-well plate), 6 technical replicates (384-well plate), and 8 replicates (1536-well plate). The fluorescence intensity was measured with an EnVision Multilabel reader as described above. The *Z′*-factor was determined with the following equation.

$$Z' = 1 - \frac{3\mathrm{SD}(100\%) + 3\mathrm{SD}(0\%)}{|\mathrm{mean}(100\%) - \mathrm{mean}(0\%)|}$$

■ ASSOCIATED CONTENT

Supporting Information

The Supporting Information is available free of charge on the ACS Publications website at DOI: 10.1021/acsomega.9b02808.

Activity of selected inhibitors against HDAC6; calculated *Z′* factors and the signal-to-noise ratio of HDAC11 and compound **1**; K_i values for listed inhibitors; the influence of BSA concentration in the assay buffer on inhibitor potency; comparison of product formation of compound **1** between the multilabel plate reader and HPLC; dose−response curves for inhibitor measurements (PDF)

■ AUTHOR INFORMATION

Corresponding Authors

*E-mail: cyril.barinka@ibt.cas.cz. Tel.: +420-325-873-777 (C.B.).

*E-mail: mike.schutkowski@biochemtech.uni-halle.de. Tel.: +49-345-5524-828 (M.S.).

ORCID

Zora Nováková: 0000-0001-9804-6346

Wolfgang Sippl: 0000-0002-5985-9261

Cyril Bařinka: 0000-0003-2751-3060

Mike Schutkowski: 0000-0003-0919-7076

Present Address

⊥Laboratory of Cell Motility, Institute of Molecular Genetics of the ASCR, v. v. i., Vídeňská 1083, Prague (G.A.).

Funding

This work was supported by grants from Deutsche Forschungsgemeinschaft (INST 271/336-1 FUGG) to M.S.Z, the Czech Science Foundation (15-19640S), the CAS (RVO: 86652036), and the project "BIOCEV" (CZ.1.05/1.1.00/02.0109) from the ERDF. We acknowledge the financial support within the funding program Open Access Publishing by the German Research Foundation (DFG).

Notes

The authors declare no competing financial interest.

■ ACKNOWLEDGMENTS

We are grateful to Ilona Kunze for technical support. We thank Prof. Dr Thomas Kiefhaber at the Martin-Luther University Halle-Wittenberg for giving us access to the single quadrupole LC−MS analyses and the MS-service facility of the Martin-Luther University Halle-Wittenberg for technical assistance during the triple-quadrupole LC−MS experiments.

■ ABBREVIATIONS

RP-HPLC,reverse-phase high-performance liquid chromatography; Abz,2-aminobenzoyl; TSA,Trichostatin A

■ REFERENCES

(1) Chen, Y.; Sprung, R.; Tang, Y.; Ball, H.; Sangras, B.; Kim, S. C.; Falck, J. R.; Peng, J.; Gu, W.; Zhao, Y. Lysine propionylation and butyrylation are novel post-translational modifications in histones. *Mol. Cell. Proteomics* **2007**, *6*, 812−819.

(2) Nishida, Y.; Rardin, M. J.; Carrico, C.; He, W.; Sahu, A. K.; Gut, P.; Najjar, R.; Fitch, M.; Hellerstein, M.; Gibson, B. W.; Verdin, E. SIRT5 Regulates both Cytosolic and Mitochondrial Protein Malonylation with Glycolysis as a Major Target. *Mol. Cell* **2015**, *59*, 321−332.

(3) Peng, C.; Lu, Z.; Xie, Z.; Cheng, Z.; Chen, Y.; Tan, M.; Luo, H.; Zhang, Y.; He, W.; Yang, K.; Zwaans, B. M. M.; Tishkoff, D.; Ho, L.; Lombard, D.; He, T.-C.; Dai, J.; Verdin, E.; Ye, Y.; Zhao, Y. The first identification of lysine malonylation substrates and its regulatory enzyme. *Mol. Cell. Proteomics* **2011**, *10*, No. M111.012658.

(4) Zhang, Z.; Tan, M.; Xie, Z.; Dai, L.; Chen, Y.; Zhao, Y. Identification of lysine succinylation as a new post-translational modification. *Nat. Chem. Biol.* **2011**, *7*, 58−63.

(5) Tan, M.; Peng, C.; Anderson, K. A.; Chhoy, P.; Xie, Z.; Dai, L.; Park, J.; Chen, Y.; Huang, H.; Zhang, Y.; Ro, J.; Wagner, G. R.; Green, M. F.; Madsen, A. S.; Schmiesing, J.; Peterson, B. S.; Xu, G.; Ilkayeva, O. R.; Muehlbauer, M. J.; Braulke, T.; Mühlhausen, C.; Backos, D. S.; Olsen, C. A.; McGuire, P. J.; Pletcher, S. D.; Lombard, D. B.; Hirschey, M. D.; Zhao, Y. Lysine glutarylation is a protein posttranslational modification regulated by SIRT5. *Cell Metabol.* **2014**, *19*, 605−617.

(6) Tan, M.; Luo, H.; Lee, S.; Jin, F.; Yang, J. S.; Montellier, E.; Buchou, T.; Cheng, Z.; Rousseaux, S.; Rajagopal, N.; Lu, Z.; Ye, Z.; Zhu, Q.; Wysocka, J.; Ye, Y.; Khochbin, S.; Ren, B.; Zhao, Y. Identification of 67 histone marks and histone lysine crotonylation as a new type of histone modification. *Cell* **2011**, *146*, 1016−1028.

(7) Xie, Z.; Zhang, Di.; Chung, D.; Tang, Z.; Huang, H.; Dai, L.; Qi, S.; Li, J.; Colak, G.; Chen, Y.; Xia, C.; Peng, C.; Ruan, H.; Kirkey, M.; Wang, D.; Jensen, L. M.; Kwon, O. K.; Lee, S.; Pletcher, S. D.; Tan, M.; Lombard, D. B.; White, K. P.; Zhao, H.; Li, J.; Roeder, R. G.; Yang, X.; Zhao, Y. Metabolic Regulation of Gene Expression by Histone Lysine β-Hydroxybutyrylation. *Mol. Cell* **2016**, *62*, 194−206.

(8) Cui, Y.; Li, X.; Lin, J.; Hao, Q.; Li, X. D. Histone Ketoamide Adduction by 4-Oxo-2-nonenal Is a Reversible Posttranslational Modification Regulated by Sirt2. *ACS Chem. Biol.* **2017**, *12*, 47−51.

(9) Galligan, J. J.; Rose, K. L.; Beavers, W. N.; Hill, S.; Tallman, K. A.; Tansey, W. P.; Marnett, L. J. Stable Histone Adduction by 4-Oxo-2-nonenal: A Potential Link between Oxidative Stress and Epigenetics. *J. Am. Chem. Soc.* **2014**, *136*, 11864−11866.

(10) Dai, L.; Peng, C.; Montellier, E.; Lu, Z.; Chen, Y.; Ishii, H.; Debernardi, A.; Buchou, T.; Rousseaux, S.; Jin, F.; Sabari, B. R.; Deng, Z.; Allis, C. D.; Ren, B.; Khochbin, S.; Zhao, Y. Lysine 2-hydroxyisobutyrylation is a widely distributed active histone mark. *Nat. Chem. Biol.* **2014**, *10*, 365−370.

DOI: 10.1021/acsomega.9b02808
ACS Omega 2019, 4, 19895−19904

(11) Anderson, K. A.; Huynh, F. K.; Fisher-Wellman, K.; Stuart, J. D.; Peterson, B. S.; Douros, J. D.; Wagner, G. R.; Thompson, J. W.; Madsen, A. S.; Green, M. F.; Sivley, R. M.; Ilkayeva, O. R.; Stevens, R. D.; Backos, D. S.; Capra, J. A.; Olsen, C. A.; Campbell, J. E.; Muoio, D. M.; Grimsrud, P. A.; Hirschey, M. D. SIRT4 Is a Lysine Deacylase that Controls Leucine Metabolism and Insulin Secretion. *Cell Metabol.* **2017**, *25*, 838−855.
(12) Wagner, G. R.; Bhatt, D. P.; O'Connell, T. M.; Thompson, J. W.; Dubois, L. G.; Backos, D. S.; Yang, H.; Mitchell, G. A.; Ilkayeva, O. R.; Stevens, R. D.; Grimsrud, P. A.; Hirschey, M. D. A Class of Reactive Acyl-CoA Species Reveals the Non-enzymatic Origins of Protein Acylation. *Cell Metabol.* **2017**, *25*, 823−837.
(13) Moellering, R. E.; Cravatt, B. F. Functional lysine modification by an intrinsically reactive primary glycolytic metabolite. *Science* **2013**, *341*, 549−553.
(14) Huang, H.; Zhang, Di.; Wang, Y.; Perez-Neut, M.; Han, Z.; Zheng, Y. G.; Hao, Q.; Zhao, Y. Lysine benzoylation is a histone mark regulated by SIRT2. *Nat. Commun.* **2018**, *9*, No. 3374.
(15) Stevenson, F. T.; Bursten, S. L.; Locksley, R. M.; Lovett, D. H. Myristyl acylation of the tumor necrosis factor alpha precursor on specific lysine residues. *J. Exp. Med.* **1992**, *176*, 1053−1062.
(16) Liu, W.; Zhou, Y.; Peng, T.; Zhou, P.; Ding, X.; Li, Z.; Zhong, H.; Xu, Y.; Chen, S.; Hang, H. C.; Shao, F. Nε-fatty acylation of multiple membrane-associated proteins by Shigella IcsB effector to modulate host function. *Nat. Microbiol.* **2018**, *3*, 996−1009.
(17) Choudhary, C.; Weinert, B. T.; Nishida, Y.; Verdin, E.; Mann, M. The growing landscape of lysine acetylation links metabolism and cell signalling. *Nat. Rev. Mol. Cell Biol.* **2014**, *15*, 536−550.
(18) Sabari, B. R.; Zhang, Di.; Allis, C. D.; Zhao, Y. Metabolic regulation of gene expression through histone acylations. *Nat. Rev. Mol. Cell Biol.* **2017**, *18*, 90−101.
(19) Seto, E.; Yoshida, M. Erasers of histone acetylation: the histone deacetylase enzymes. *Cold Spring Harbor Perspect. Biol.* **2014**, *6*, No. a018713.
(20) Kutil, Z.; Novakova, Z.; Meleshin, M.; Mikesova, J.; Schutkowski, M.; Barinka, C. Histone Deacetylase 11 Is a Fatty-Acid Deacylase. *ACS Chem. Biol.* **2018**, *13*, 685−693.
(21) Moreno-Yruela, C.; Galleano, I.; Madsen, A. S.; Olsen, C. A. Histone Deacetylase 11 Is an ε-N-Myristoyllysine Hydrolase. *Cell Chem. Biol.* **2018**, *25*, 849−856.
(22) Cao, J.; Sun, L.; Aramsangtienchai, P.; Spiegelman, N. A.; Zhang, X.; Huang, W.; Seto, E.; Lin, H. HDAC11 regulates type I interferon signaling through defatty-acylation of SHMT2. *Proc. Natl. Acad. Sci. U.S.A.* **2019**, *116*, 5487−5492.
(23) McCullough, C. E.; Marmorstein, R. Molecular Basis for Histone Acetyltransferase Regulation by Binding Partners, Associated Domains, and Autoacetylation. *ACS Chem. Biol.* **2016**, *11*, 632−642.
(24) Sun, L.; Marin de Evsikova, C.; Bian, K.; Achille, A.; Telles, E.; Pei, H.; Seto, E. Programming and Regulation of Metabolic Homeostasis by HDAC11. *EBioMedicine* **2018**, *33*, 157−168.
(25) Huang, J.; Wang, L.; Dahiya, S.; Beier, U. H.; Han, R.; Samanta, A.; Bergman, J.; Sotomayor, E. M.; Seto, E.; Kozikowski, A. P.; Hancock, W. W. Histone/protein deacetylase 11 targeting promotes Foxp3+ Treg function. *Sci. Rep.* **2017**, *7*, No. 8626.
(26) Martin, M. W.; Lee, J. Y.; Lancia, D. R.; Ng, P. Y.; Han, B.; Thomason, J. R.; Lynes, M. S.; Marshall, C. G.; Conti, C.; Collis, A.; Morales, M. A.; Doshi, K.; Rudnitskaya, A.; Yao, L.; Zheng, X. Discovery of novel N-hydroxy-2-arylisoindoline-4-carboxamides as potent and selective inhibitors of HDAC11. *Bioorg. Med. Chem. Lett.* **2018**, *28*, 2143−2147.
(27) in Son, S.; Cao, J.; Zhu, C.-L.; Miller, S. P.; Lin, H. Activity-Guided Design of HDAC11-Specific Inhibitors. *ACS Chem. Biol.* **2019**, No. 292.
(28) Fan, Y.; Scriba, G. K. E. Electrophoretically mediated microanalysis assay for sirtuin enzymes. *Electrophoresis* **2010**, *31*, 3874−3880.
(29) Ohla, S.; Beyreiss, R.; Scriba, G. K. E.; Fan, Y.; Belder, D. An integrated on-chip sirtuin assay. *Electrophoresis* **2010**, *31*, 3263−3267.
(30) Blackwell, L.; Norris, J.; Suto, C. M.; Janzen, W. P. The use of diversity profiling to characterize chemical modulators of the histone deacetylases. *Life Sci.* **2008**, *82*, 1050−1058.
(31) Liu, Y.; Gerber, R.; Wu, J.; Tsuruda, T.; McCarter, J. D. High-throughput assays for sirtuin enzymes: a microfluidic mobility shift assay and a bioluminescence assay. *Anal. Biochem.* **2008**, *378*, 53−59.
(32) Khan, A. N.; Lewis, P. N. Unstructured conformations are a substrate requirement for the Sir2 family of NAD-dependent protein deacetylases. *J. Biol. Chem.* **2005**, *280*, 36073−36078.
(33) Du, J.; Zhou, Y.; Su, X.; Yu, J. J.; Khan, S.; Jiang, H.; Kim, J.; Woo, J.; Kim, J. H.; Choi, B. H.; He, B.; Chen, W.; Zhang, S.; Cerione, R. A.; Auwerx, J.; Hao, Q.; Lin, H. Sirt5 is a NAD-dependent protein lysine demalonylase and desuccinylase. *Science* **2011**, *334*, 806−809.
(34) Marcotte, P. A.; Richardson, P. L.; Richardson, P. R.; Guo, J.; Barrett, L. W.; Xu, N.; Gunasekera, A.; Glaser, K. B. Fluorescence assay of SIRT protein deacetylases using an acetylated peptide substrate and a secondary trypsin reaction. *Anal. Biochem.* **2004**, *332*, 90−99.
(35) Tanner, K. G.; Landry, J.; Sternglanz, R.; Denu, J. M. Silent information regulator 2 family of NAD- dependent histone/protein deacetylases generates a unique product, 1-O-acetyl-ADP-ribose. *Proc. Natl. Acad. Sci. U.S.A.* **2000**, *97*, 14178−14182.
(36) Jackson, M. D.; Denu, J. M. Structural identification of 2′- and 3′-O-acetyl-ADP-ribose as novel metabolites derived from the Sir2 family of beta -NAD+-dependent histone/protein deacetylases. *J. Biol. Chem.* **2002**, *277*, 18535−18544.
(37) Khan, A. N.; Lewis, P. N. Use of substrate analogs and mutagenesis to study substrate binding and catalysis in the Sir2 family of NAD-dependent protein deacetylases. *J. Biol. Chem.* **2006**, *281*, 11702−11711.
(38) Borra, M. T.; Denu, J. M. Quantitative Assays for Characterization of the Sir2 Family of NAD+-Dependent Deacetylases. In *Chromatin and Chromatin Remodeling Enzymes*; Allis, C. D., Ed.; Elsevier: Amsterdam, 2004; pp 171−187.
(39) McDonagh, T.; Hixon, J.; DiStefano, P. S.; Curtis, R.; Napper, A. D. Microplate filtration assay for nicotinamide release from NAD using a boronic acid resin. *Methods* **2005**, *36*, 346−350.
(40) Hoffmann, K.; Heltweg, B.; Jung, M. Improvement and validation of the fluorescence-based histone deacetylase assay using an internal standard. *Arch. Pharm.* **2001**, *334*, 248−252.
(41) Rye, P. T.; Frick, L. E.; Ozbal, C. C.; Lamarr, W. A. Advances in label-free screening approaches for studying sirtuin-mediated deacetylation. *J. Biomol. Screening* **2011**, *16*, 1217−1226.
(42) Fischer, F.; Gertz, M.; Suenkel, B.; Lakshminarasimhan, M.; Schutkowski, M.; Steegborn, C. Sirt5 deacylation activities show differential sensitivities to nicotinamide inhibition. *PLoS One* **2012**, *7*, No. e45098.
(43) Gurard-Levin, Z. A.; Kilian, K. A.; Kim, J.; Bähr, K.; Mrksich, M. Peptide arrays identify isoform-selective substrates for profiling endogenous lysine deacetylase activity. *ACS Chem. Biol.* **2010**, *5*, 863−873.
(44) Gurard-Levin, Z. A.; Kim, J.; Mrksich, M. Combining mass spectrometry and peptide arrays to profile the specificities of histone deacetylases. *ChemBioChem* **2009**, *10*, 2159−2161.
(45) Kuo, H.-Y.; DeLuca, T. A.; Miller, W. M.; Mrksich, M. Profiling deacetylase activities in cell lysates with peptide arrays and SAMDI mass spectrometry. *Anal. Chem.* **2013**, *85*, 10635−10642.
(46) Castaneda, C. A.; Lopez, J. E.; Joseph, C. G.; Scholle, M. D.; Mrksich, M.; Fierke, C. A. Active Site Metal Identity Alters Histone Deacetylase 8 Substrate Selectivity: A Potential Novel Regulatory Mechanism. *Biochemistry* **2017**, *56*, 5663−5670.
(47) Kutil, Z.; Skultetyova, L.; Rauh, D.; Meleshin, M.; Snajdr, I.; Novakova, Z.; Mikesova, J.; Pavlicek, J.; Hadzima, M.; Baranova, P.; Havlinova, B.; Majer, P.; Schutkowski, M.; Barinka, C. The unraveling of substrate specificity of histone deacetylase 6 domains using acetylome peptide microarrays and peptide libraries. *FASEB J.* **2019**, *33*, 4035−4045.

DOI: 10.1021/acsomega.9b02808
ACS Omega 2019, 4, 19895−19904

(48) Rauh, D.; Fischer, F.; Gertz, M.; Lakshminarasimhan, M.; Bergbrede, T.; Aladini, F.; Kambach, C.; Becker, C. F. W.; Zerweck, J.; Schutkowski, M.; Steegborn, C. An acetylome peptide microarray reveals specificities and deacetylation substrates for all human sirtuin isoforms. *Nat. Commun.* **2013**, *4*, No. 2327.
(49) Robers, M. B.; Loh, C.; Carlson, C. B.; Yang, H.; Frey, E. A.; Hermanson, S. B.; Bi, K. Measurement of the cellular deacetylase activity of SIRT1 on p53 via LanthaScreen technology. *Mol. BioSyst.* **2011**, *7*, 59−66.
(50) Dudek, J. M.; Horton, R. A. TR-FRET biochemical assays for detecting posttranslational modifications of p53. *J. Biomol. Screening* **2010**, *15*, 569−575.
(51) Machleidt, T.; Robers, M. B.; Hermanson, S. B.; Dudek, J. M.; Bi, K. TR-FRET cellular assays for interrogating posttranslational modifications of histone H3. *J. Biomol. Screening* **2011**, *16*, 1236−1246.
(52) Degorce, F.; Card, A.; Soh, S.; Trinquet, E.; Knapik, G. P.; Xie, B. HTRF: A technology tailored for drug discovery - a review of theoretical aspects and recent applications. *Curr. Chem. Genomics* **2009**, *3*, 22−32.
(53) Inoue, A.; Fujimoto, D. Enzymatic deacetylation of histone. *Biochem. Biophys. Res. Commun.* **1969**, *36*, 146−150.
(54) Kölle, D.; Brosch, G.; Lechner, T.; Lusser, A.; Loidl, P. Biochemical methods for analysis of histone deacetylases. *Methods* **1998**, *15*, 323−331.
(55) Taunton, J.; Hassig, C. A.; Schreiber, S. L. A mammalian histone deacetylase related to the yeast transcriptional regulator Rpd3p. *Science* **1996**, *272*, 408−411.
(56) Milne, J. C.; Lambert, P. D.; Schenk, S.; Carney, D. P.; Smith, J. J.; Gagne, D. J.; Jin, L.; Boss, O.; Perni, R. B.; Vu, C. B.; Bemis, J. E.; Xie, R.; Disch, J. S.; Ng, P. Y.; Nunes, J. J.; Lynch, A. V.; Yang, H.; Galonek, H.; Israelian, K.; Choy, W.; Iffland, A.; Lavu, S.; Medvedik, O.; Sinclair, D. A.; Olefsky, J. M.; Jirousek, M. R.; Elliott, P. J.; Westphal, C. H. Small molecule activators of SIRT1 as therapeutics for the treatment of type 2 diabetes. *Nature* **2007**, *450*, 712−716.
(57) Wolfson, N. A.; Pitcairn, C. A.; Sullivan, E. D.; Joseph, C. G.; Fierke, C. A. An enzyme-coupled assay measuring acetate production for profiling histone deacetylase specificity. *Anal. Biochem.* **2014**, *456*, 61−69.
(58) Fatkins, D. G.; Monnot, A. D.; Zheng, W. Nepsilon-thioacetyllysine: a multi-facet functional probe for enzymatic protein lysine Nepsilon-deacetylation. *Bioorg. Med. Chem. Lett.* **2006**, *16*, 3651−3656.
(59) Heltweg, B.; Dequiedt, F.; Verdin, E.; Jung, M. Nonisotopic substrate for assaying both human zinc and NAD+-dependent histone deacetylases. *Anal. Biochem.* **2003**, *319*, 42−48.
(60) Toro, T. B.; Watt, T. J. KDAC8 substrate specificity quantified by a biologically relevant, label-free deacetylation assay. Protein science: a publication of the Protein. *Society* **2015**, *24*, 2020−2032.
(61) Baba, R.; Hori, Y.; Mizukami, S.; Kikuchi, K. Development of a fluorogenic probe with a transesterification switch for detection of histone deacetylase activity. *J. Am. Chem. Soc.* **2012**, *134*, 14310−14313.
(62) Baba, R.; Hori, Y.; Kikuchi, K. Intramolecular long-distance nucleophilic reactions as a rapid fluorogenic switch applicable to the detection of enzymatic activity. *Chem. - Eur. J.* **2015**, *21*, 4695−4702.
(63) Rooker, D. R.; Klyubka, Y.; Gautam, R.; Tomat, E.; Buccella, D. Peptide-Based Fluorescent Probes for Deacetylase and Decrotonylase Activity: Toward a General Platform for Real-Time Detection of Lysine Deacylation. *ChemBioChem* **2018**, *19*, 496−504.
(64) Liu, X.; Xiang, M.; Tong, Z.; Luo, F.; Chen, W.; Liu, F.; Wang, F.; Yu, R.-Q.; Jiang, J.-H. Activatable Fluorescence Probe via Self-Immolative Intramolecular Cyclization for Histone Deacetylase Imaging in Live Cells and Tissues. *Anal. Chem.* **2018**, *90*, 5534−5539.
(65) Xie, Y.; Ge, J.; Lei, H.; Peng, B.; Zhang, H.; Wang, D.; Pan, S.; Chen, G.; Chen, L.; Wang, Y.; Hao, Q.; Yao, S. Q.; Sun, H. Fluorescent Probes for Single-Step Detection and Proteomic Profiling of Histone Deacetylases. *J. Am. Chem. Soc.* **2016**, *138*, 15596−15604.
(66) Yu, C.; Wu, Y.; Zeng, F.; Li, X.; Shi, J.; Wu, S. Hyperbranched polyester-based fluorescent probe for histone deacetylase via aggregation-induced emission. *Biomacromolecules* **2013**, *14*, 4507−4514.
(67) Dhara, K.; Hori, Y.; Baba, R.; Kikuchi, K. A fluorescent probe for detection of histone deacetylase activity based on aggregation-induced emission. *Chem. Commun.* **2012**, *48*, 11534−11536.
(68) Minoshima, M.; Matsumoto, T.; Kikuchi, K. Development of a fluorogenic probe based on a DNA staining dye for continuous monitoring of the histone deacetylase reaction. *Anal. Chem.* **2014**, *86*, 7925−7930.
(69) Han, Y.; Li, H.; Hu, Y.; Li, P.; Wang, H.; Nie, Z.; Yao, S. Time-resolved luminescence biosensor for continuous activity detection of protein acetylation-related enzymes based on DNA-sensitized terbium(III) probes. *Anal. Chem.* **2015**, *87*, 9179−9185.
(70) Halley, F.; Reinshagen, J.; Ellinger, B.; Wolf, M.; Niles, A. L.; Evans, N. J.; Kirkland, T. A.; Wagner, J. M.; Jung, M.; Gribbon, P.; Gul, S. A bioluminogenic HDAC activity assay: validation and screening. *J. Biomol. Screening* **2011**, *16*, 1227−1235.
(71) Dose, A.; Jost, J. O.; Spieß, A. C.; Henklein, P.; Beyermann, M.; Schwarzer, D. Facile synthesis of colorimetric histone deacetylase substrates. *Chem. Commun.* **2012**, *48*, 9525−9527.
(72) Riester, D.; Hildmann, C.; Grünewald, S.; Beckers, T.; Schwienhorst, A. Factors affecting the substrate specificity of histone deacetylases. *Biochem. Biophys. Res. Commun.* **2007**, *357*, 439−445.
(73) Wegener, D.; Hildmann, C.; Riester, D.; Schober, A.; Meyer-Almes, F.-J.; Deubzer, H. E.; Oehme, I.; Witt, O.; Lang, S.; Jaensch, M.; Makarov, V.; Lange, C.; Busse, B.; Schwienhorst, A. Identification of novel small-molecule histone deacetylase inhibitors by medium-throughput screening using a fluorigenic assay. *Biochem. J.* **2008**, *413*, 143−150.
(74) Ciossek, T.; Julius, H.; Wieland, H.; Maier, T.; Beckers, T. A homogeneous cellular histone deacetylase assay suitable for compound profiling and robotic screening. *Anal. Biochem.* **2008**, *372*, 72−81.
(75) Wegener, D.; Hildmann, C.; Riester, D.; Schwienhorst, A. Improved fluorogenic histone deacetylase assay for high-throughput-screening applications. *Anal. Biochem.* **2003**, *321*, 202−208.
(76) Wegener, D.; Wirsching, F.; Riester, D.; Schwienhorst, A. A fluorogenic histone deacetylase assay well suited for high-throughput activity screening. *Chem. Biol.* **2003**, *10*, 61−68.
(77) Bradner, J. E.; West, N.; Grachan, M. L.; Greenberg, E. F.; Haggarty, S. J.; Warnow, T.; Mazitschek, R. Chemical phylogenetics of histone deacetylases. *Nat. Chem. Biol.* **2010**, *6*, 238−243.
(78) Lahm, A.; Paolini, C.; Pallaoro, M.; Nardi, M. C.; Jones, P.; Neddermann, P.; Sambucini, S.; Bottomley, M. J.; Lo Surdo, P.; Carfí, A.; Koch, U.; Francesco, R.; de; Steinkühler, C.; Gallinari, P. Unraveling the hidden catalytic activity of vertebrate class IIa histone deacetylases. *Proc. Natl. Acad. Sci. U.S.A.* **2007**, *104*, 17335−17340.
(79) Toro, T. B.; Bryant, J. R.; Watt, T. J. Lysine Deacetylases Exhibit Distinct Changes in Activity Profiles Due to Fluorophore Conjugation of Substrates. *Biochemistry* **2017**, *56*, 4549−4558.
(80) Kawaguchi, M.; Ikegawa, S.; Ieda, N.; Nakagawa, H. A Fluorescent Probe for Imaging Sirtuin Activity in Living Cells, Based on One-Step Cleavage of the Dabcyl Quencher. *ChemBioChem* **2016**, *17*, 1961−1967.
(81) Schuster, S.; Roessler, C.; Meleshin, M.; Zimmermann, P.; Simic, Z.; Kambach, C.; Schiene-Fischer, C.; Steegborn, C.; Hottiger, M. O.; Schutkowski, M. A continuous sirtuin activity assay without any coupling to enzymatic or chemical reactions. *Sci. Rep.* **2016**, *6*, No. 22643.
(82) Jiang, H.; Khan, S.; Wang, Y.; Charron, G.; He, B.; Sebastian, C.; Du, J.; Kim, R.; Ge, E.; Mostoslavsky, R.; Hang, H. C.; Hao, Q.; Lin, H. SIRT6 regulates TNF-α secretion through hydrolysis of long-chain fatty acyl lysine. *Nature* **2013**, *496*, 110−113.
(83) Neelarapu, R.; Holzle, D. L.; Velaparthi, S.; Bai, H.; Brunsteiner, M.; Blond, S. Y.; Petukhov, P. A. Design, synthesis, docking, and biological evaluation of novel diazide-containing

DOI: 10.1021/acsomega.9b02808
ACS Omega 2019, 4, 19895−19904

isoxazole- and pyrazole-based histone deacetylase probes. *J. Med. Chem.* **2011**, *54*, 4350−4364.
(84) Yu, C.-W.; Chang, P.-T.; Hsin, L.-W.; Chern, J.-W. Quinazolin-4-one derivatives as selective histone deacetylase-6 inhibitors for the treatment of Alzheimer's disease. *J. Med. Chem.* **2013**, *56*, 6775−6791.
(85) Salvador, L. A.; Park, H.; Al-Awadhi, F. H.; Liu, Y.; Kim, B.; Zeller, S. L.; Chen, Q.-Y.; Hong, J.; Luesch, H. Modulation of Activity Profiles for Largazole-Based HDAC Inhibitors through Alteration of Prodrug Properties. *ACS Med. Chem. Lett.* **2014**, *5*, 905−910.
(86) Yao, Y.; Tu, Z.; Liao, C.; Wang, Z.; Li, S.; Yao, H.; Li, Z.; Jiang, S. Discovery of Novel Class I Histone Deacetylase Inhibitors with Promising in Vitro and in Vivo Antitumor Activities. *J. Med. Chem.* **2015**, *58*, 7672−7680.
(87) Chen, Y.; Wang, X.; Xiang, W.; He, L.; Tang, M.; Wang, F.; Wang, T.; Yang, Z.; Yi, Y.; Wang, H.; Niu, T.; Zheng, L.; Lei, L.; Li, X.; Song, H.; Chen, L. Development of Purine-Based Hydroxamic Acid Derivatives: Potent Histone Deacetylase Inhibitors with Marked in Vitro and in Vivo Antitumor Activities. *J. Med. Chem.* **2016**, *59*, 5488−5504.
(88) Spiegelman, N. A.; Price, I. R.; Jing, H.; Wang, M.; Yang, M.; Cao, J.; Hong, J. Y.; Zhang, X.; Aramsangtienchai, P.; Sadhukhan, S.; Lin, H. Direct Comparison of SIRT2 Inhibitors: Potency, Specificity, Activity-Dependent Inhibition, and On-Target Anticancer Activities. *ChemMedChem* **2018**, *13*, 1890−1894.
(89) Kannan, S.; Melesina, J.; Hauser, A.-T.; Chakrabarti, A.; Heimburg, T.; Schmidtkunz, K.; Walter, A.; Marek, M.; Pierce, R. J.; Romier, C.; Jung, M.; Sippl, W. Discovery of inhibitors of Schistosoma mansoni HDAC8 by combining homology modeling, virtual screening, and in vitro validation. *J. Chem. Inf. Model.* **2014**, *54*, 3005−3019.
(90) Riester, D.; Wegener, D.; Hildmann, C.; Schwienhorst, A. Members of the histone deacetylase superfamily differ in substrate specificity towards small synthetic substrates. *Biochem. Biophys. Res. Commun.* **2004**, *324*, 1116−1123.
(91) Roessler, C.; Nowak, T.; Pannek, M.; Gertz, M.; Nguyen, G. T. T.; Scharfe, M.; Born, I.; Sippl, W.; Steegborn, C.; Schutkowski, M. Chemical probing of the human sirtuin 5 active site reveals its substrate acyl specificity and peptide-based inhibitors. *Angew. Chem., Int. Ed.* **2014**, *53*, 10728−10732.
(92) Zhang, J. H. A Simple Statistical Parameter for Use in Evaluation and Validation of High Throughput Screening Assays. *J. Biomol. Screening* **1999**, *4*, 67−73.
(93) Auzzas, L.; Larsson, A.; Matera, R.; Baraldi, A.; Deschênes-Simard, B.; Giannini, G.; Cabri, W.; Battistuzzi, G.; Gallo, G.; Ciacci, A.; Vesci, L.; Pisano, C.; Hanessian, S. Non-natural macrocyclic inhibitors of histone deacetylases: design, synthesis, and activity. *J. Med. Chem.* **2010**, *53*, 8387−8399.
(94) Zhou, N.; Moradei, O.; Raeppel, S.; Leit, S.; Frechette, S.; Gaudette, F.; Paquin, I.; Bernstein, N.; Bouchain, G.; Vaisburg, A.; Jin, Z.; Gillespie, J.; Wang, J.; Fournel, M.; Yan, P. T.; Trachy-Bourget, M.-C.; Kalita, A.; Lu, A.; Rahil, J.; MacLeod, A. R.; Li, Z.; Besterman, J. M.; Delorme, D. Discovery of N-(2-aminophenyl)-4-(4-pyridin-3-ylpyrimidin-2-ylamino)methylbenzamide (MGCD0103), an orally active histone deacetylase inhibitor. *J. Med. Chem.* **2008**, *51*, 4072−4075.
(95) Arts, J.; King, P.; Marïen, A.; Floren, W.; Beliën, A.; Janssen, L.; Pilatte, I.; Roux, B.; Decrane, L.; Gilissen, R.; Hickson, I.; Vreys, V.; Cox, E.; Bol, K.; Talloen, W.; Goris, I.; Andries, L.; Du Jardin, M.; Janicot, M.; Page, M.; van Emelen, K.; Angibaud, P. JNJ-26481585, a novel "second-generation" oral histone deacetylase inhibitor, shows broad-spectrum preclinical antitumoral activity. *Clin. Cancer Res.* **2009**, *15*, 6841−6851.
(96) Novotny-Diermayr, V.; Sangthongpitag, K.; Hu, C. Y.; Wu, X.; Sausgruber, N.; Yeo, P.; Greicius, G.; Pettersson, S.; Liang, A. L.; Loh, Y. K.; Bonday, Z.; Goh, K. C.; Hentze, H.; Hart, S.; Wang, H.; Ethirajulu, K.; Wood, J. M. SB939, a novel potent and orally active histone deacetylase inhibitor with high tumor exposure and efficacy in mouse models of colorectal cancer. *Mol. Cancer Ther.* **2010**, *9*, 642−652.
(97) Yang, Z.; Wang, T.; Wang, F.; Niu, T.; Liu, Z.; Chen, X.; Long, C.; Tang, M.; Cao, D.; Wang, X.; Xiang, W.; Yi, Y.; Ma, L.; You, J.; Chen, L. Discovery of Selective Histone Deacetylase 6 Inhibitors Using the Quinazoline as the Cap for the Treatment of Cancer. *J. Med. Chem.* **2016**, *59*, 1455−1470.
(98) Santo, L.; Hideshima, T.; Kung, A. L.; Tseng, J.-C.; Tamang, D.; Yang, M.; Jarpe, M.; van Duzer, J. H.; Mazitschek, R.; Ogier, W. C.; Cirstea, D.; Rodig, S.; Eda, H.; Scullen, T.; Canavese, M.; Bradner, J.; Anderson, K. C.; Jones, S. S.; Raje, N. Preclinical activity, pharmacodynamic, and pharmacokinetic properties of a selective HDAC6 inhibitor, ACY-1215, in combination with bortezomib in multiple myeloma. *Blood* **2012**, *119*, 2579−2589.
(99) Muthyala, R.; Shin, W. S.; Xie, J.; Sham, Y. Y. Discovery of 1-hydroxypyridine-2-thiones as selective histone deacetylase inhibitors and their potential application for treating leukemia. *Bioorg. Med. Chem. Lett.* **2015**, *25*, 4320−4324.
(100) Marek, L.; Hamacher, A.; Hansen, F. K.; Kuna, K.; Gohlke, H.; Kassack, M. U.; Kurz, T. Histone deacetylase (HDAC) inhibitors with a novel connecting unit linker region reveal a selectivity profile for HDAC4 and HDAC5 with improved activity against chemoresistant cancer cells. *J. Med. Chem.* **2013**, *56*, 427−436.
(101) Cincinelli, R.; Musso, L.; Giannini, G.; Zuco, V.; Cesare, M.; de; Zunino, F.; Dallavalle, S. Influence of the adamantyl moiety on the activity of biphenylacrylohydroxamic acid-based HDAC inhibitors. *Eur. J. Med. Chem.* **2014**, *79*, 251−259.
(102) Yung-Chi, C.; Prusoff, W. H. Relationship between the inhibition constant (KI) and the concentration of inhibitor which causes 50 per cent inhibition (I50) of an enzymatic reaction. *Biochem. Pharm.* **1973**, *22*, 3099−3108.

DOI: 10.1021/acsomega.9b02808
ACS Omega 2019, 4, 19895−19904